Journal of Structural Engineering and Geotechnics,
2 (2), 51-65, Summer 2012

The Evaluation of Nonlinear Response of Structures to Near-Fault Ground Motions and the Comparison of Results with Near-Fault Simulated Records

M. Askari[*a], H. Aghabarati[b]

[a] *Graduate Student, Qazvin Branch, Islamic Azad University, Qazvin, Iran*
[b] *Assistant Professor, Qazvin Branch, Islamic Azad University, Qazvin, Iran*

Received 9 August2012, Accepted 7 October2012

Abstract

Near-fault ground motions have caused very much damage in the vicinity of seismic sources during recent earthquakes. It is well known that under specific circumstances, intensive ground shakings near fault ruptures may be characterized by short-duration impulsive motions. This pulse-type motion is generally particular to the forward direction, where the fault rupture propagates towards the site at a velocity close to shear wave velocity. Ground motions affected by directivity focusing at near-field stations contain distinct pulses in acceleration, velocity and displacement histories. These ground motions can generate much higher base shears, inter-story drifts and roof displacements as compared to far-fault ground motions. Since structures under the effect of destructive earthquakes enter an inelastic phase, so the study of inelastic behavior of structures under the effect of such earthquakes seems to be important. This study examined maximum acceleration, velocity, displacement of the roof mass center, inter-story drifts and base shears of building in inelastic state at moment steel frame buildings designed on the basis of buildings design code against earthquake (2800 Standard, the third edition) under the near-fault records and the comparison of these parameters with the simulated ones. The results indicate that the maximum demand of drift of stories, acceleration, velocity, displacement of roof mass center and inelastic base shear and the way of hinge formation in non-linear state under the near-fault records is the same as simulated records in short buildings. Moreover, the more the height of structure becomes, the more different the behavior of structure becomes and the response is affected by more faults or errors.

Key Words: Near-fault ground motion,Near-fault simulated records, Non-liner the histories analysis

1. Introduction

Near-fault ground motions have caused much damage in the vicinity of seismic sources during recent earthquakes (Northridge 1994, Kobe 1995, and Imperial Valley 1979). It is well known that under specific circumstances, intensive ground shakings near fault ruptures may be characterized by short-duration impulsive motions. This pulse-type motion is generally particular to the forward direction, where the fault rupture propagates towards the site at a velocity close to shear wave velocity [1]. The radiation pattern of the shear dislocation on the fault causes this large pulse of motion to be oriented in the direction perpendicular to the fault. Thus, the fault-normal component of the motion may be more severe than the fault-parallel component [2]. Ground motions affected by directivity focusing at near-field stations contain distinct pulses in the acceleration, velocity, and displacement histories. In a strike-slip earthquake, if the rupture propagates in the direction of the recording station, the coherently travelling long-period waves result in large values of ground velocities and displacements in the fault-normal direction. Because the high-frequency waves are less likely to travel in a coherent manner, the ground accelerations are relatively unaffected by directivity focusing. The effect of directivity focusing is most pronounced on displacements, less on velocities, and least on accelerations. Directivity focusing can also occur for dip-slip faulting, although the conditions required are met less readily than for strike-slip faulting [3]. In addition, near-fault earthquake records are rich in high frequencies because the short travel distance of the seismic waves would not allow high-frequency content to be damped as is normally observed in the far-field records[4].Permanent ground displacement due to the tectonic deformation field of the earthquake, named as fling-step, is another important characteristic of near-fault earthquake records. Fling-step displacement occur sin the direction of fault slip; mtherefore, for strike-slip earthquakes, it is not

*Corresponding Author Email:m.askari@qiau.ac.ir

strongly coupled with the directivity pulses while for dip-slip earthquakes, a fling-step pulse may coincide with directivity pulses and produce stronger low-frequency motions [5,6]. Among the aforementioned characteristics, i.e., directivity pulses, high-frequency content, and fling-step, the first one has attracted much attention as a critical subject in the design of structures in the near-fault zone. The special response characteristics of near-fault ground motions deserve further scrutiny. The development (or improvement) of design guidelines for structures close to a seismic source requires a thorough understanding of near-fault response phenomena [7]. The peculiar structural response to the large pulse of motion in the vicinity of seismic source, a.k.a. "fling", was pointed out by Mahin et al. (1976) and Bertero et al. (1978) after the 1971 San Fernando earthquake. They noted that the building of the Olive View Medical Center suffered extensive damage caused by a severe pulse, which they identified as characteristic of near-fault ground motions. They concluded that the damage was the result of only a few large displacement excursions rather than of a large number of oscillations as in ordinary ground motions. They also concluded that short period structures designed to code requirements could experience very large ductility demands when subjected to near-fault ground motions, and thus special design precautions should be taken for structures located near active faults [8, 9]. Anderson and Naeim (1984) showed that near-fault ground motions with pulses can induce dramatically high response in fixed-base buildings [10]. Hall et al., in their study of buildings subjected to artificially generated pulse-like ground motions, indicated that the demands imposed by the displacement pulses in the near-fault ground motions can far exceed the capacity of flexible high-rise and base-isolated buildings designed to current standards. Also they employed wave propagation theory to study the response of a continuous shear building to pulse-type ground motions. They warned about the damaging effects of near-fault ground motions and the inadequacy of current code provisions to address the problem effectively [11].Makris categorized long-period pulses in near-fault ground motions into three types, each represented by a distinct tri-geometric function [12]. Chopra and Chintanapakdee, in their preliminary investigation, concluded that the response spectrum analysis is accurate for engineering applications and should be preferred over the drift spectrum [13]. Bozorgnia and Mahin (1998) used idealized rectangular acceleration pulses and showed the efficiency of this synthetic model to represent inelastic response of structures against real near-fault records [14].Baker (2007) used wavelet analysis to extract directivity velocity pulses. He used the ratio of the extracted pulse amplitude to that of the original record to develop a quantitative criterion for classification of near-fault ground motions [15]. Also Sigurdsson discusses the characteristics of near-fault ground motions, and explains how they are related to rupture geometry, site properties and its location relative to source and forward directivity effects [16]. Besides, Champion and Liel quantify the effects of forward directivity on collapse risk through incremental dynamic analysis of building simulation models that are capable of capturing the key aspects of strength and stiffness degradation associated with structural collapse [17]. In Go to 's thesis, the seismic response of a bridge designed according to the current Japanese Design Specifications was evaluated when it is subjected to near-field ground motions recorded during the 1995 Kobe earthquake and far-field ground motions recorded during the 2011 Great East Japan earthquake. For this purpose, a series of nonlinear dynamic response analysis was conducted and the seismic performance of the bridge was verified in terms of its displacement and ductility demand [18].

The paper intends to study the maximum acceleration, velocity and displacement of the roof mass center, inter-story drifts and base shears of buildings in inelastic state at moment steel frame buildings with different heights under the near-fault and simulated records which is on the basis of buildings design code against earthquake. The results reveal that the obtained amounts under the near-fault records and simulated ones in shorter buildings are close and by the increase in height and higher modes effects, the accuracy of the work decreases and a more different behavior is observed. Besides, structure response experiences more errors.

One of the most important applications of the study is to save money and time in achieving a desired response in inelastic state of moment steel frame buildings. The creativity of the present paper, in comparison with the previous ones, is that after studying the acceleration records, pulses with large and effective amplitude are extracted and sine equations that have amplitudes close to the amplitudes of acceleration record are replaced with those pulses and make the simulated records. It can be used in engineering works at long time analyses instead of real acceleration records and hence responses with very high accuracy are obtained**.**

2. Modeling of frames in SAP2000 and assumptions of the study

The major aim of the study is the comparison of near-fault records with pulse-type simulated records. To this end, a non-linear time history analysis in SAP2000 v.12.0.0 and a simple plan (Fig. 1) with 4 different heights of 4,8,12 and 16 stories is used that all of these structures are at both directions of intermediate moment steel frame. For simplifying and better comparison of the study, firstly the structure is designed on the basis of Iran steel code [19], its loading is performed on the basis of Iran loading code [20] and seismic loading is done on the basis of Iran 2800 seismic code [21]. This method is applied to better comparison of the records in structures since the height of the structure can be a very good parameter for comparing the structure behavior in different kinds of various earthquakes. In this study, 7 near-fault earthquakes are

used that partial distance of seismography station to superficial seismic center is less than 15 Km which are given in Table 1 and are compared with simulated records that the way of simulation of these records is explained in next section. Besides, inelastic deformations are admissible only at the end of story beams and at both ends of story columns. So, the mechanism of base plastic hinge under lateral loads involves all stories. The mechanism represented in Fig. 2, indicates structures that follow the necessary steps from common codes "weak beam- strong column". In the study, plastic hinges used at beams and columns are from a hysteresis non-linear model and are taken from Tables 3-5 of publication 360 Iran [22]. On the whole, the following assumptions are used in general design of structure model:

The building is built on a region with high seismicity like Tehran; Hence the PGA of the design base earthquake is 0.35g. In order to decrease the effect of soil-structure interaction, it was assumed that the studied structures are rested on a hard soil. The lateral bearing system was steel intermediate moment resisting frame in both directions. The dead loads of 6KN/m^2 and live load of 2KN/m^2 were distributed on all of the floors.

All of the structural elements were made of mild steel kind by ($F_y = 2400\frac{Kg}{cm^2}$) and($F_u = 3700\frac{Kg}{cm^2}$).

The buildings are regular in plan and height. It should be noted that all earthquakes are applied to the structural models in one direction.

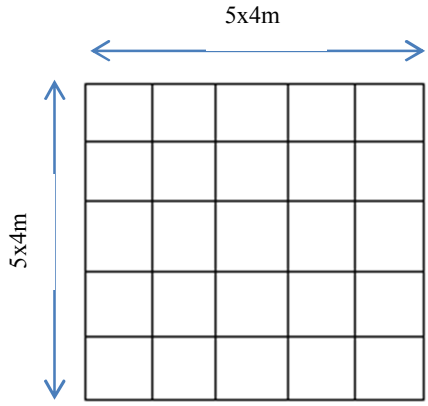

Fig 1.The studied buildings plan

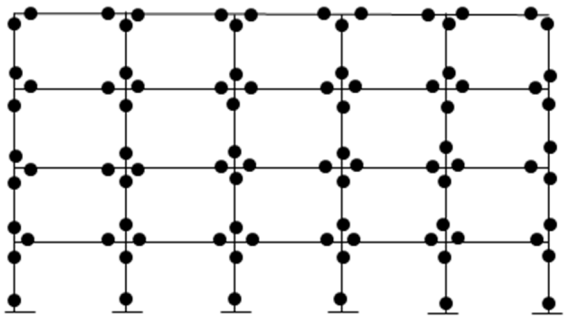

Fig 2. The Location of probable plastic hinges in buildings

3. Simulation of near-fault acceleration record

In this part, the simulations of the above-mentioned near-fault records are explained and $\{\sin(\frac{\pi t}{T_D})\}$ equation is used for simulation. The equations are arranged so that the closest near-fault record amplitude is obtained. It should be mentioned that only large and effective pulses of near-fault records which are less than 10 seconds aresimulated and the simulation of ineffective pulses are avoided.Moreover, small acceleration pulses are simulated before the above-mentioned large pulses since these small pulses can affect structure behavior. In the study, as much as possible, small pulses of about 0.1g take part in simulation before large pulses. In Fig. 3, the acceleration simulation of 7 near-fault records is clearly represented.

Table 1. The studied near-fault and simulated acceleration record

Record	Station	PGA(g) Near-Fault	PGA(g) Simulated
Erzincan	Erzincan	0.52	0.4
Imperial Valley	El Centro Array 5	0.52	0.25
Kobe	Takatori	0.61	0.5
LomaPrieta	Los Gatos Presentation Center	0.563	0.55
Northridge	Rinaldi Receiving Station	0.84	0.8
Parkfield	Cholame#2	0.476	0.35
SuperstationHills	ParachuteTestSite	0.46	0.4

Erzincan:

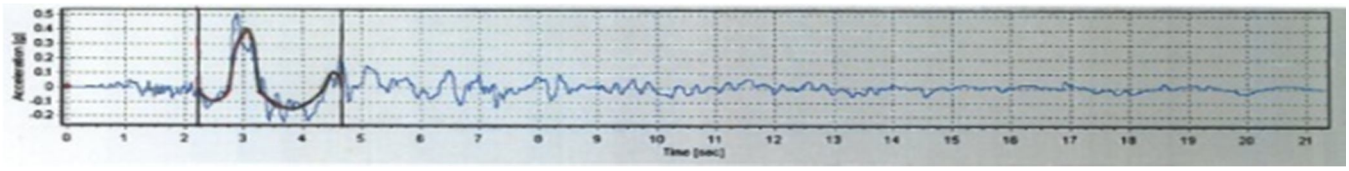

Acceleration

$Ug = -0.1g\ Sin(\pi t/T_D1)$ $0 \le t \le T_D1$ $T_D1 = 0.5$ sec

$Ug = -0.4g\ Sin(\pi t/T_D2+\pi/6)$ $T_D1 \le t \le T_D2+T_D1$ $T_D2 = 0.6$ sec

$Ug = -0.15g\ Sin(\pi t/T_D3+9\pi/10)$ $T_D2+T_D1 \le t \le T_D3+T_D2+T_D1$ $T_D3 = 1$ sec

$Ug = -0.1g\ Sin(\pi t/T_D4)$ $T_D3+T_D2+T_D1 \le t \le T_D4+T_D3+T_D2+T_D1$ $T_D4 = 0.3$ sec

Imperial Valley:

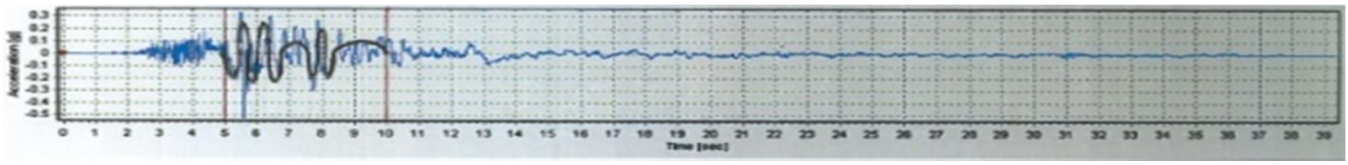

Acceleration

$Ug = -0.2g\ Sin(\pi t/T_D1)$ $0 \le t \le T_D1$ $T_D1 = 0.4$ sec

$Ug = -0.25g\ Sin(\pi t/T_D2-\pi/3)$ $T_D1 \le t \le 4T_D2+T_D1$ $T_D2 = 0.3$ sec

$Ug = -0.1g\ Sin(\pi t/T_D3-6\pi/10)$ $4T_D2+T_D1 \le t \le T_D3+4T_D2+T_D1$ $T_D3 = 1$ sec

$Ug = -0.2g\ Sin(\pi t/T_D4-2\pi/5)$ $T_D3+4T_D2+T_D1 \le t \le 3T_D4+T_D3+4T_D2+T_D1$ $T_D4 = 0.25$sec

$Ug = 0.1g\ Sin(\pi t/T_D5-\pi/33)$ $3T_D4+T_D3+4T_D2+T_D1 \le t \le T_D5+3T_D4+T_D3+4T_D2+T_D1$ $T_D5 = 1.65$sec

Kobe:

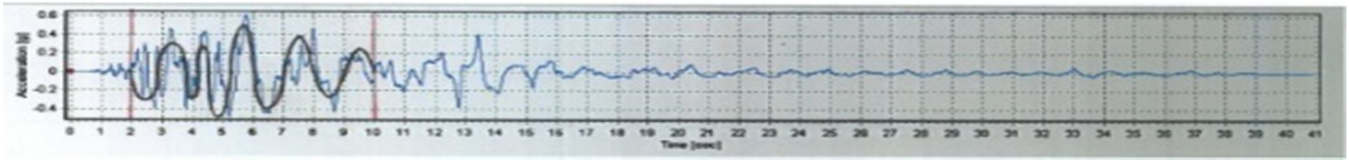

Acceleration

$Ug = -0.3g\ Sin(\pi t/T_D1)$ $0 \le t \le 2T_D1$ $T_D1 = 0.9$ sec

$Ug = -0.3g\ Sin(\pi t/T_D2-8\pi/7)$ $2T_D1 \le t \le 2T_D2+2T_D1$ $T_D2 = 0.35$ sec

$Ug = 0.5g\ Sin(\pi t/T_D3-\pi/3)$ $2T_D2+2T_D1 \le t \le 2T_D3+2T_D2+2T_D1$ $T_D3 = 0.75$ sec

$Ug = -0.4g\ Sin(\pi t/T_D4)$ $2T_D3+2T_D2+2T_D1 \le t \le 2T_D4+2T_D3+2T_D2+2T_D1$ $T_D4 = 0.25$sec

$Ug = -0.25g\ Sin(\pi t/T_D5)$ $2T_D4+2T_D3+2T_D2+2T_D1 \le t \le 2T_D5+2T_D4+2T_D3+2T_D2+2T_D1$ $T_D5 = 1$ sec

Fig 3: Simulated accelerations of the study

LomaPrieta:

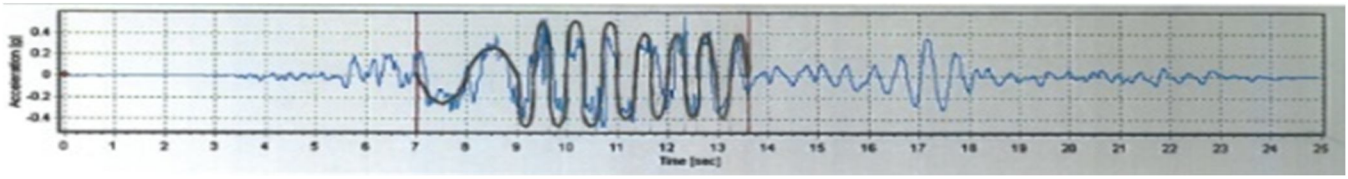

Acceleration

$Ug = -0.25g\ Sin(\pi t/T_D1)$ $0 \le t \le 2T_D1$ $T_D1 = 1$ sec

$Ug = -0.55g\ Sin(\pi t/T_D2-54\pi/13)$ $2T_D1 \le t \le 6T_D2+2T_D1$ $T_D2 = 0.325$ sec

$Ug = -0.4g\ Sin(\pi t/T_D2-54\pi/13)$ $6T_D2+2T_D1 \le t \le 14T_D2+2T_D1$ $T_D2 = 0.325$ sec

Northridge:

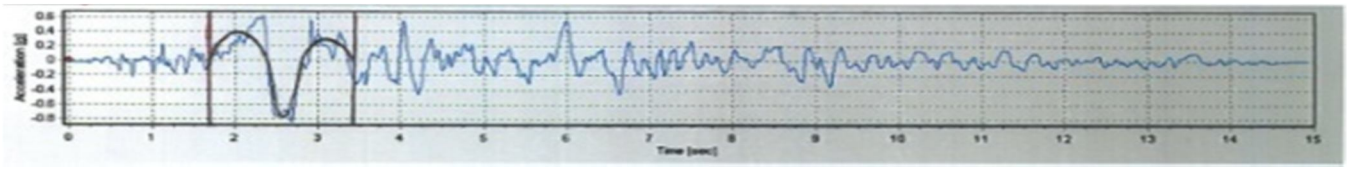

Acceleration

$Ug = 0.4g\ Sin(\pi t/T_D1)$ $0 \le t \le T_D1$ $T_D1 = 0.7$ sec

$Ug = 0.8g\ Sin(\pi t/T_D2)$ $T_D1 \le t \le T_D2+T_D1$ $T_D2 = 0.4$ sec

$Ug = 0.3g\ Sin(\pi t/T_D3)$ $T_D2+T_D1 \le t \le T_D3+T_D2+T_D1$ $T_D3 = 0.6$ sec

Parkfield:

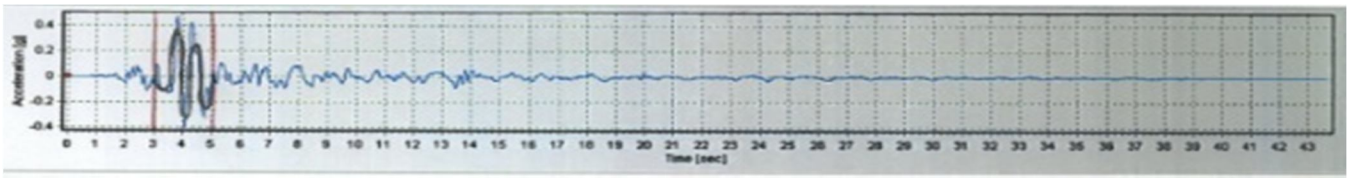

Acceleration

$Ug = -0.1g\ Sin(\pi t/T_D1)$ $0 \le t \le T_D1$ $T_D1 = 0.5$ sec

$Ug = 0.35g\ Sin(\pi t/T_D2-\pi/3)$ $T_D1 \le t \le 2T_D2+T_D1$ $T_D2 = 0.375$ sec

$Ug = 0.25g\ Sin(\pi t/T_D2-\pi/3)$ $2T_D2+T_D1 \le t \le 4T_D2+T_D1$ $T_D2 = 0.375$ sec

Superstation Hills:

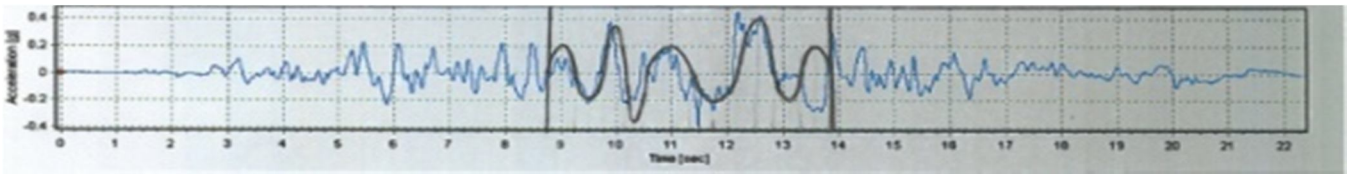

Acceleration

$Ug = 0.2g\ Sin(\pi t/T_D1)$ $0 \le t \le 2T_D1$ $T_D1 = 0.5$ sec

$Ug = 0.35g\ Sin(\pi t/T_D2-\pi/2)$ $2T_D1 \le t \le 2T_D2+2T_D1$ $T_D2 = 0.4$ sec

$Ug = 0.2g\ Sin(\pi t/T_D3-\pi/4)$ $2T_D2+2T_D1 \le t \le 2T_D3+2T_D2+2T_D1$ $T_D3 = 0.8$ sec

$Ug = 0.4g\ Sin(\pi t/T_D4-6\pi/7)$ $2T_D3+2T_D2+2T_D1 \le t \le T_D4+2T_D3+2T_D2+2T_D1$ $T_D4 = 0.7$sec

$Ug = 0.2g\ Sin(\pi t/T_D5-\pi/5)$ $T_D4+2T_D3+2T_D2+2T_D1 \le t \le 2T_D5+T_D4+2T_D3+2T_D2+2T_D1$ $T_D5 = 0.5$ sec

Fig.3.(Continue) Simulated accelerations of the study

4. Fourier spectra of near-fault and simulated acceleration records

In order to ensure maximum precision in this study, Fourier spectra of 7 near-fault acceleration records and simulated ones are extracted. Fig. 4 illustrates the Fourier spectra of near-fault and simulated earthquakes and compares them with each other. As shown in the Figure, the Fourier spectrum of near-fault records and simulated ones are approximately close to each other and their peak amounts are a little before or after 1 Hz frequency.

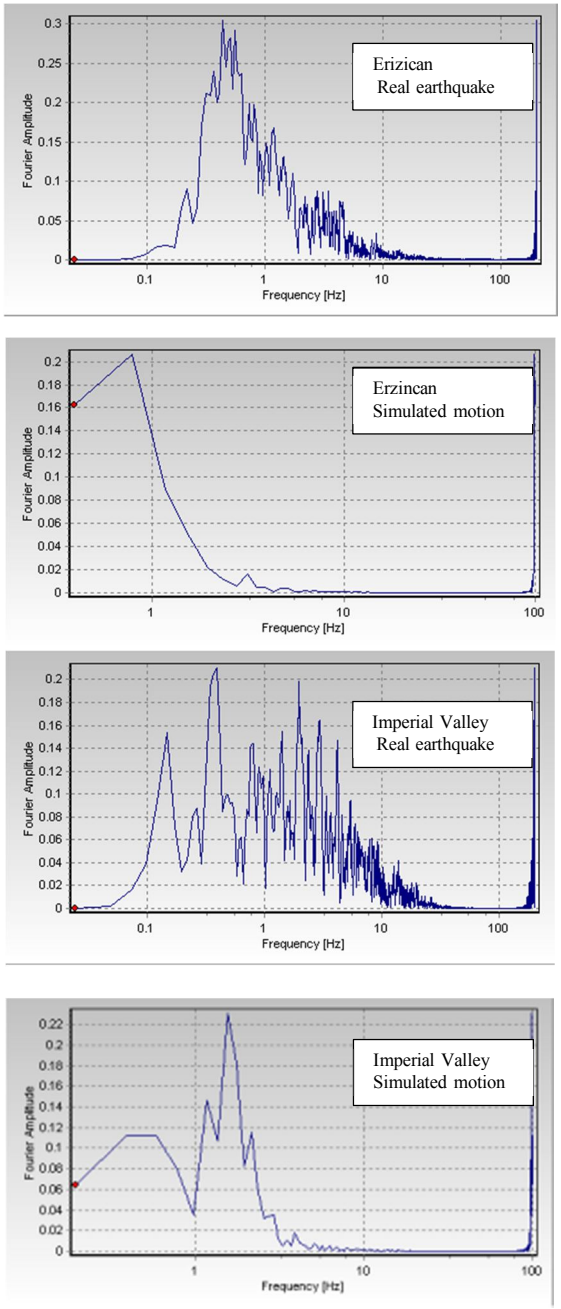

Fig.4. Fourier spectra of near-fault and simulated acceleration records

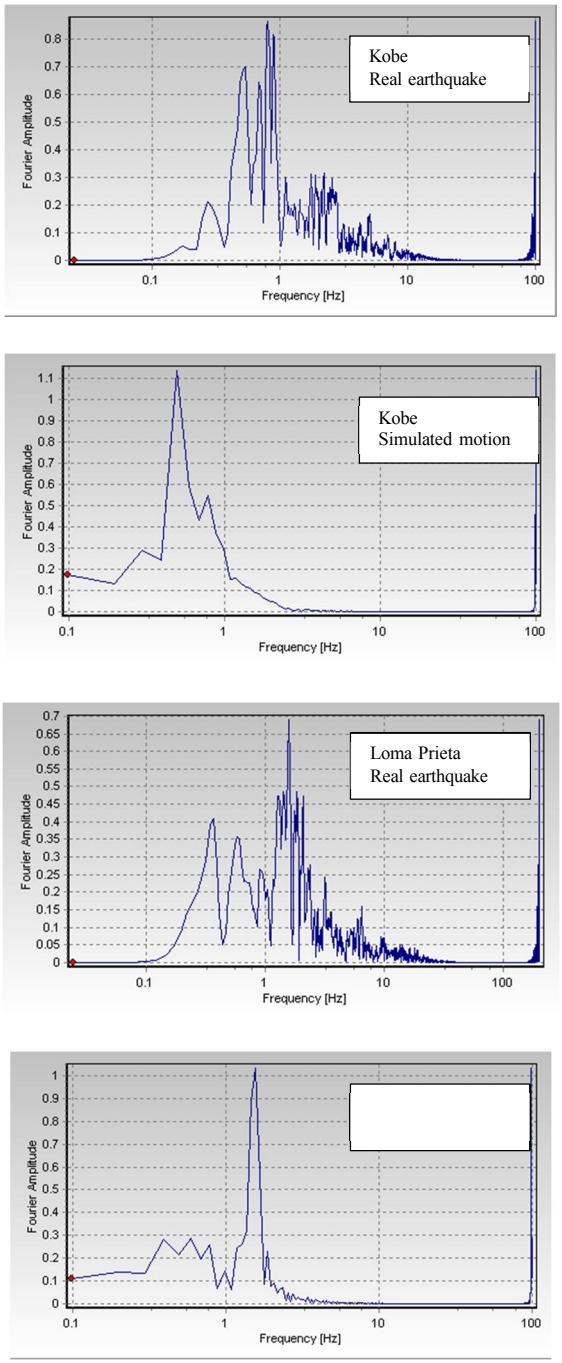

Fig.4. (Continue) Fourier spectra of near-fault and simulated acceleration records

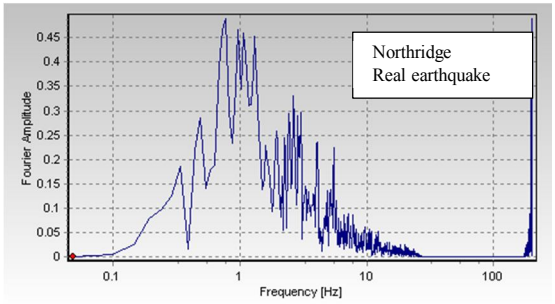

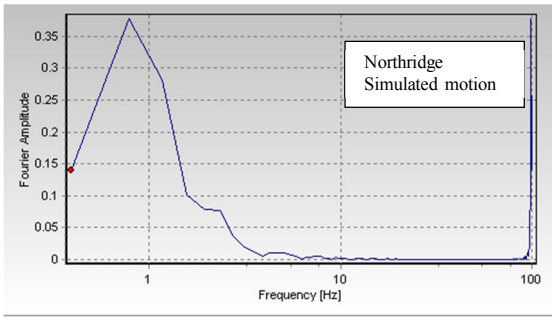

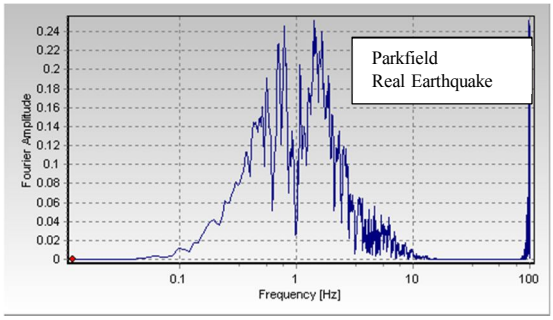

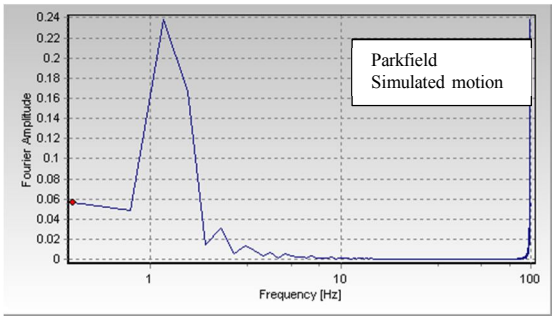

Fig 4. Fourier spectra of near-fault and simulated acceleration records

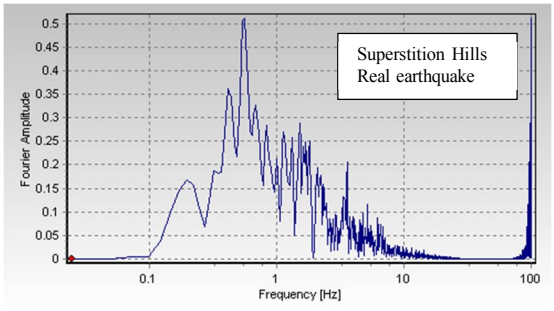

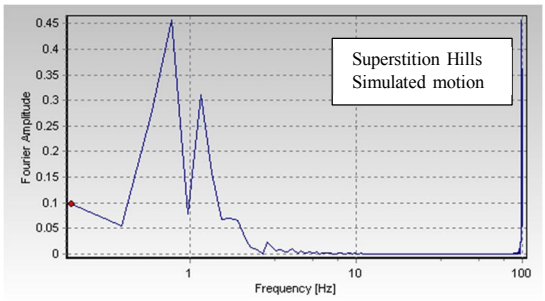

Fig 4. Fourier spectra of near-fault and simulated acceleration records

5. Maximum inelastic displacement, velocity and acceleration of roof mass center in studied structures

After non-linear dynamic analysis, the results of displacement, velocity and acceleration of roof mass center at 4 studied buildings for 7 near-fault and simulated records are represented in Figs.5 to 7. As is clearly specified in the diagrams, maximum inelastic displacement, velocity and acceleration in near-fault and simulated records are similar in most records; and are slightly different in some records which can be ignored. The reason for this difference can be the structure without displacement, velocity and acceleration at the beginning of simulated records and all these parameters are zero while the structure under near-fault records at the onset of starting simulated records, has displacement, velocity and acceleration; and such values of displacement, velocity and acceleration change the structure behavior during the record time. The average of maximum records displacement for 4,8,12 and 16-story buildings under near-fault records is respectively 27.53, 42.24, 57.86 and 64.35 cm and such criterion under simulated records is respectively 29.13, 45.85, 54.25 and 55.9. Also, the average of maximum structure inelastic velocity under near-fault records in 4-story building is 1.31m/s, in 8-story building is 1.85m/s, in 12-story building is 2.03m/s and in 16-story building is 2.11m/s. Besides, this velocity under simulated records in 4-story building is 1.41m/s, in 8-story building is 1.88m/s, in 12-story building is 1.85m/s and in 16-story building are 2.04m/s. The average of maximum inelastic

acceleration in 4-story and 8-story buildings under near-fault records is more than the average of maximum inelastic acceleration in 12-story and 16-story buildings. This is also true in simulated records but with less accuracy that is specified to some extent. However, the case will be true when the accuracy in the way of simulation in records (acceleration record) is high and if an acceleration record is not simulated with high accuracy and precision, the response obtained by simulated records may be completely incorrect or with very low precision.

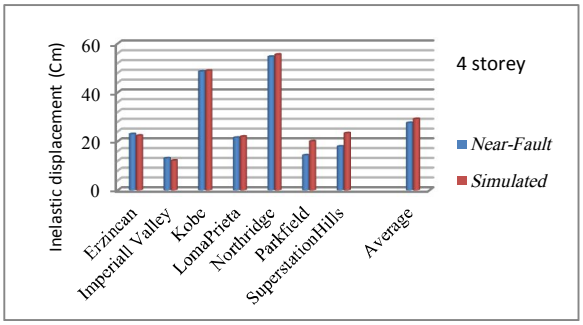

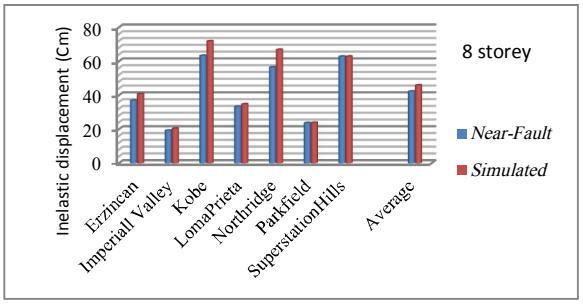

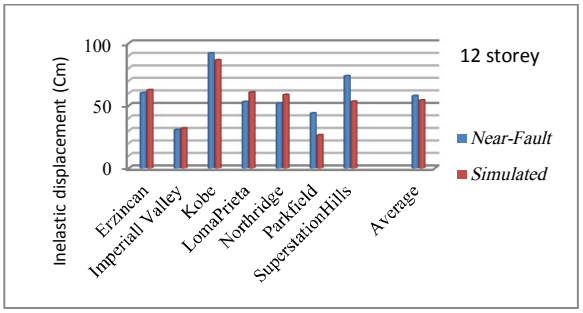

Fig.5. Maximum inelastic displacement of roof mass center (cm) under near-fault and simulated records

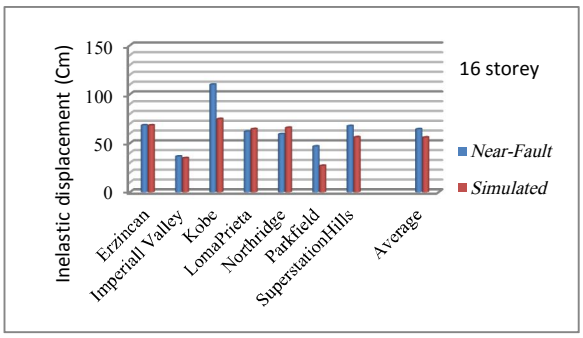

Fig. 5. (Continue) Maximum inelastic displacement of roof mass center (cm) under near-fault and simulated records

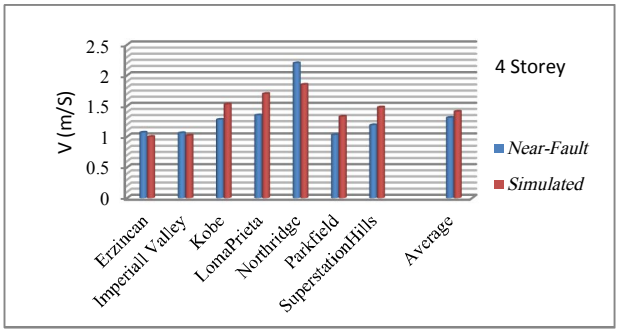

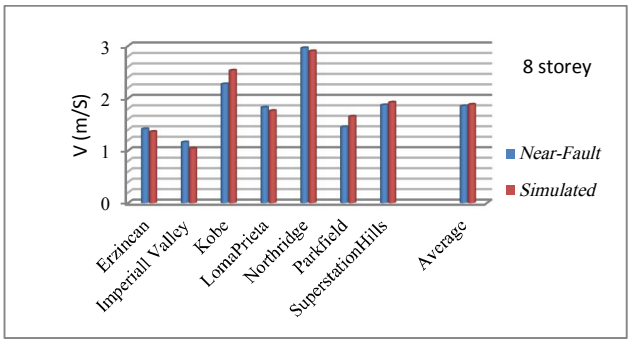

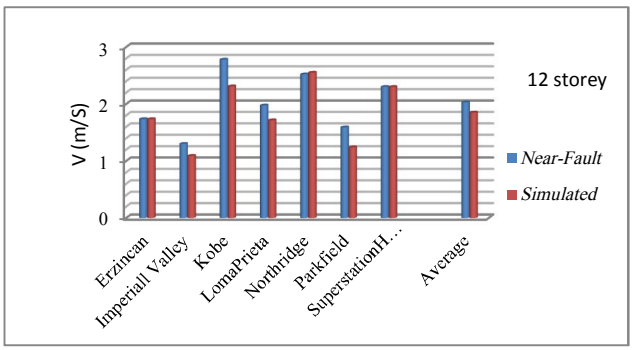

Fig.6. Maximum inelastic velocity of roof mass center ($\frac{m}{s}$) under near-fault and simulated records

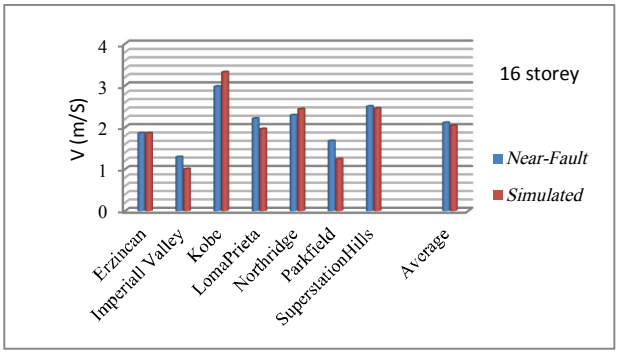

Fig.6. (Continue) Maximum inelastic velocity of roof mass center ($\frac{m}{s}$) under near-fault and simulated records

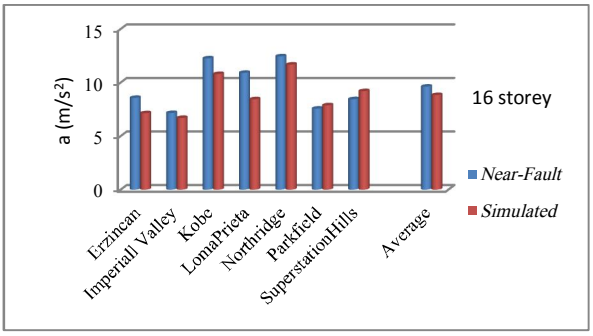

Fig.7. (Continue) Maximum inelastic acceleration of roof mass center ($\frac{m}{s^2}$) under near-fault and simulated records

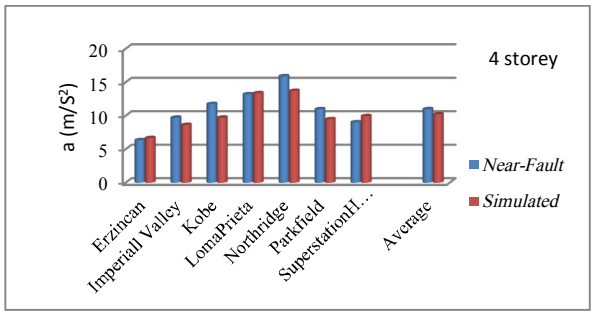

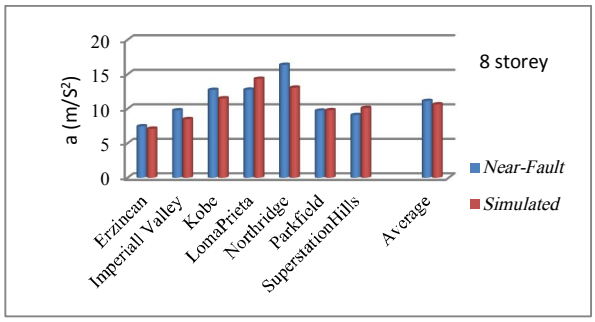

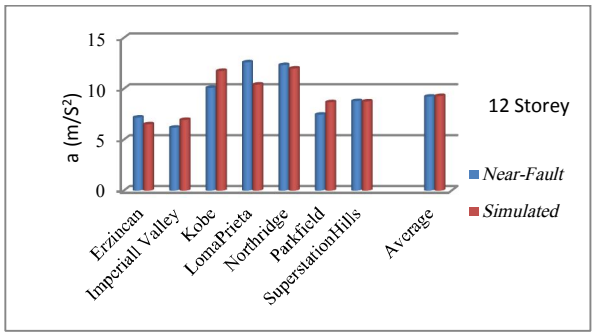

Fig.7. Maximum inelastic acceleration of roof mass center ($\frac{m}{s^2}$) under near-fault and simulated records

6. Maximum drift ratio of stories

One of the major structure responses to earthquake whether in static analyses or in dynamic analyses, is controlling the maximum drift of structure stories. Figures 8 to 12 represent maximum drift ratios of stories for 4,8,12 and 16-story buildings under 7 near-fault and 7 simulated records. As is shown in the following figures, in 4-story buildings, the drift ratio of stories under both records increases in second and third stories and decreases in fourth story; and the difference in both records is very low. In 8-story buildings, the drift ratio primarily increases and finally decreases. But we cannot say on which story it has the highest value. Also the error value increases compared to a 4-story building. In a 12-story building, the drift ratio is in the form of M but the error value also grows and the drift ratio in some records possesses a more different response. In a 16-story building, the behavior is to some extent similar to a 12-story building but it has less regularity and is affected by more errors.

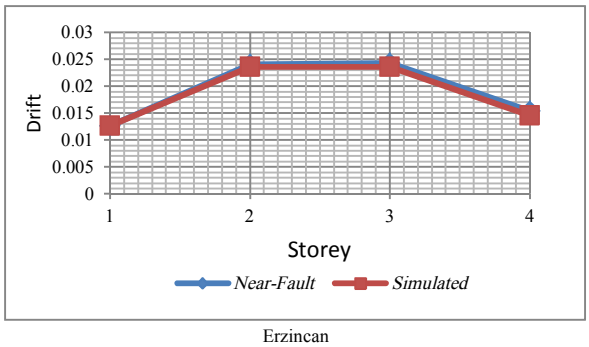

Fig 8. Maximum drift of stories for 4-story building under 7 near-fault and 7 simulated records

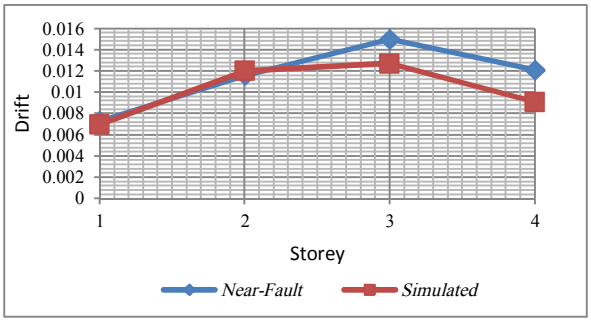

Imperial Valley

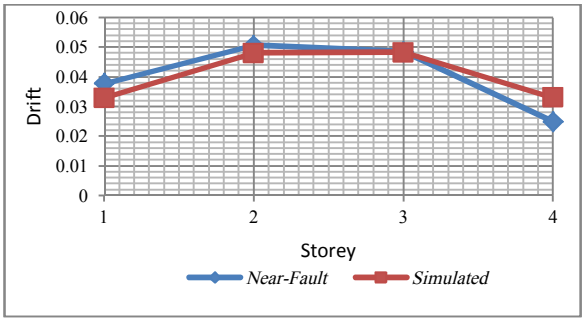

Kobe

Fig 8.(Continue). Maximum drift of stories for 4-story building under 7 near-fault and 7 simulated records

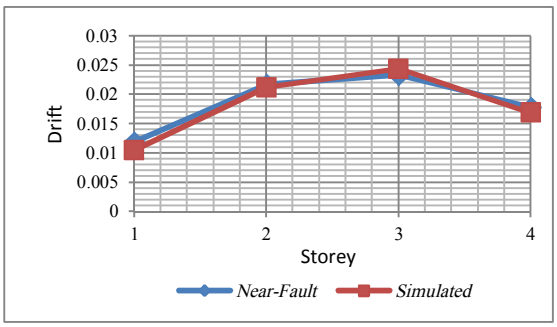

LomaPrieta

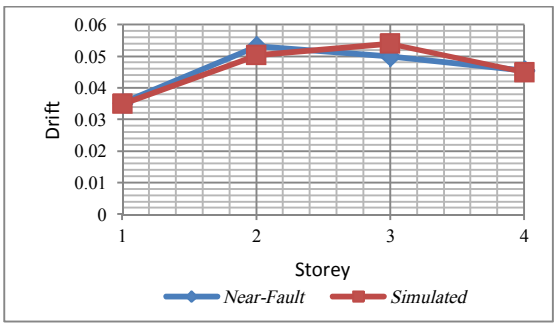

Northridge

Fig 9. Maximum drift of stories for 4-story building under 7 near-fault and 7 simulated records

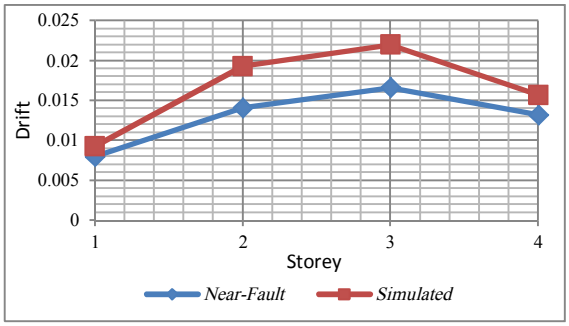

Parkfield

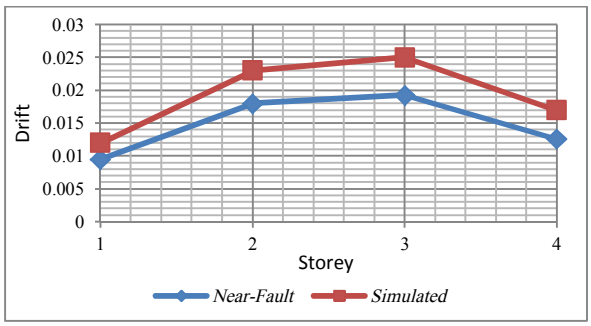

SuperstationHills

Fig 9.(Continue) Maximum drift of stories for 4-story building under 7 near-fault and 7 simulated records

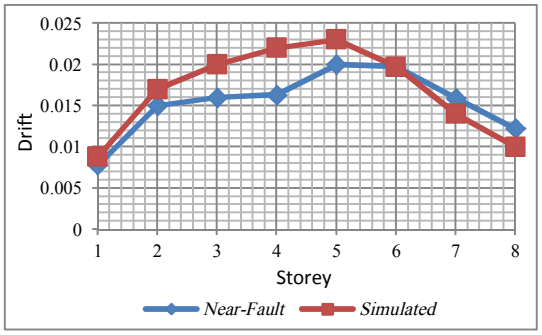

Erzincan

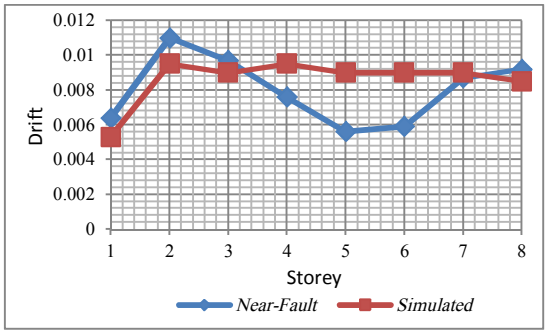

Imperial Valley

Fig.10. Maximum drift of stories for 8-story building under 7 near-fault and 7 simulated records

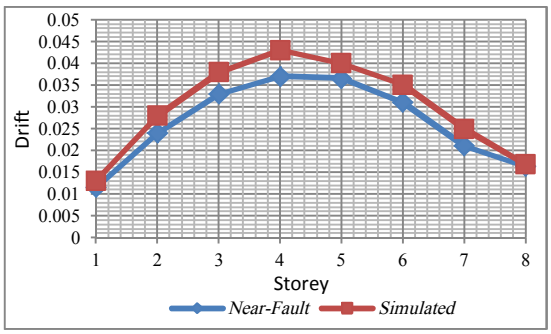

Kobe

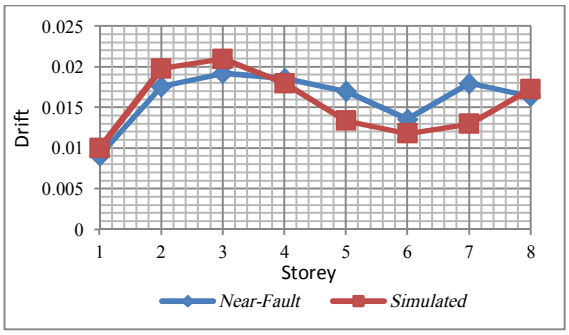

LomaPrieta

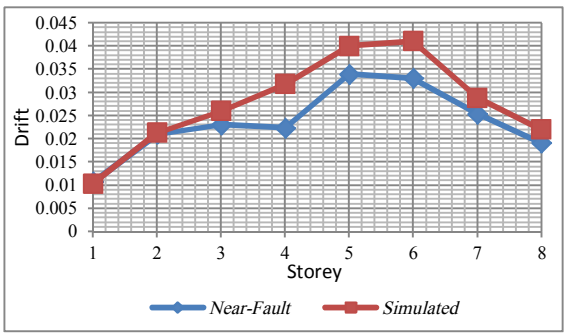

Northridge

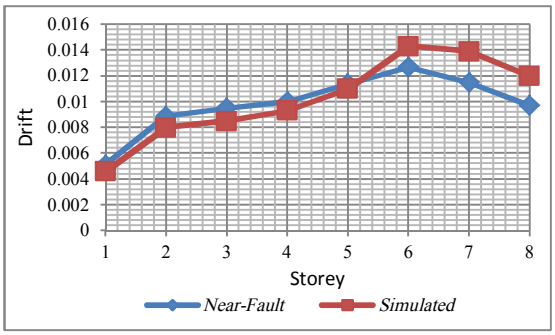

Parkfield

Fig.10. (Continue) Maximum drift of stories for 8-story building under 7 near-fault and 7 simulated records

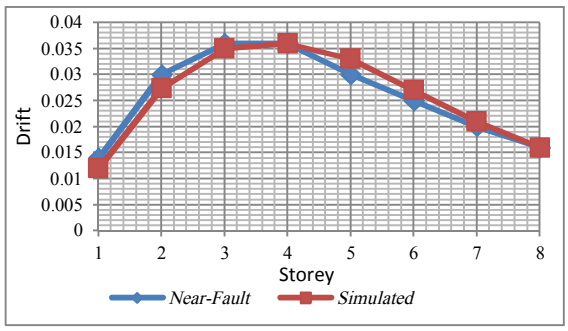

SuperstationHills

Fig.10. (Continue) Maximum drift of stories for 8-story building under 7 near-fault and 7 simulated records

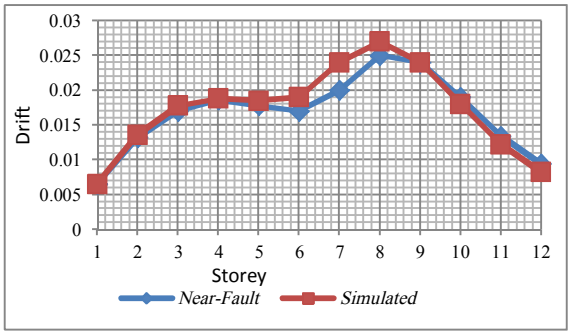

Erzincan

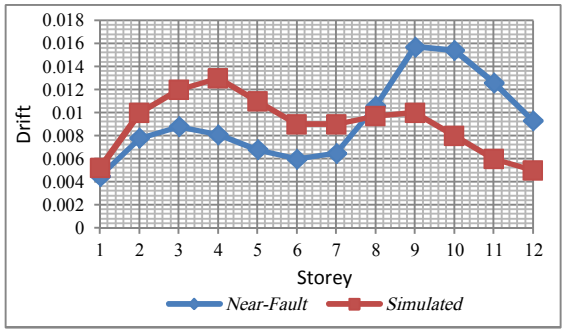

Imperial Valley

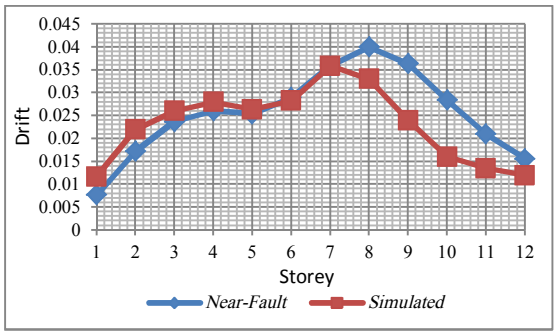

Kobe

Fig.11. Maximum drift of stories for 12-story building under 7 near-fault and 7 simulated records

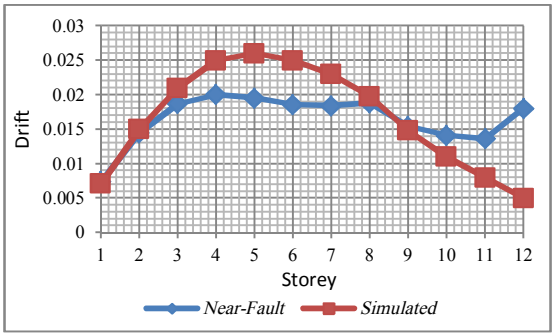

LomaPrieta

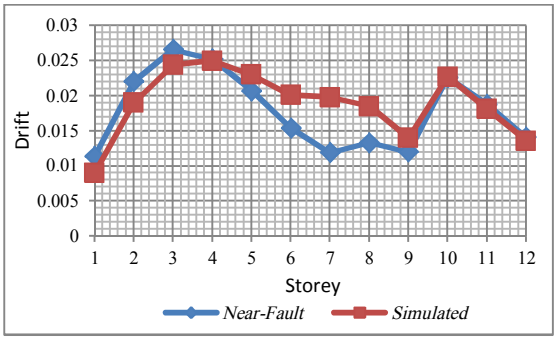

Northridge

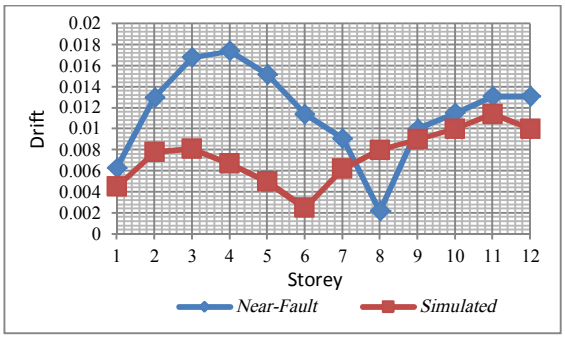

Parkfield

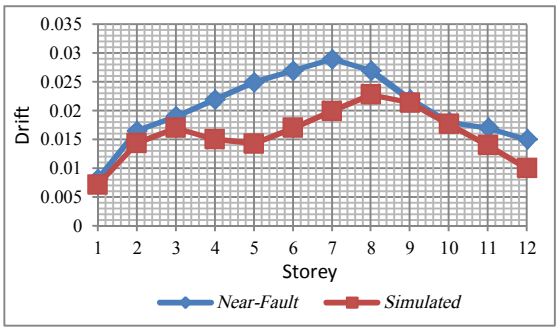

SuperstationHills

Fig.11. (Continue) Maximum drift of stories for 12-story building under 7 near-fault and 7 simulated records

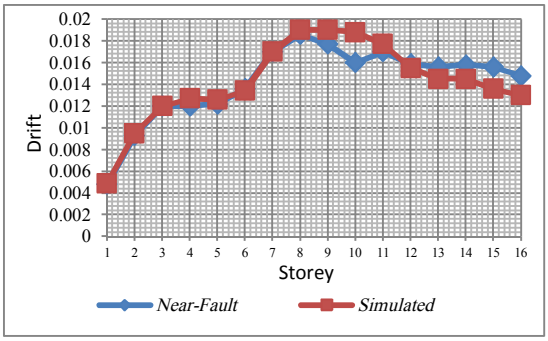

Erzincan

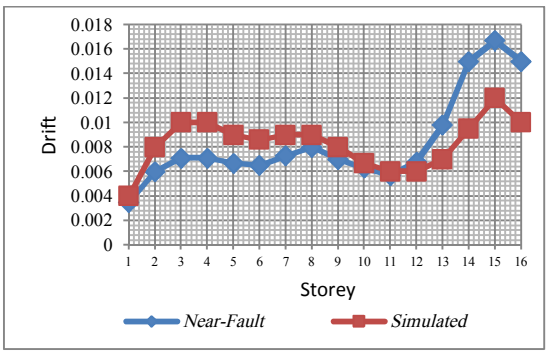

Imperial Valley

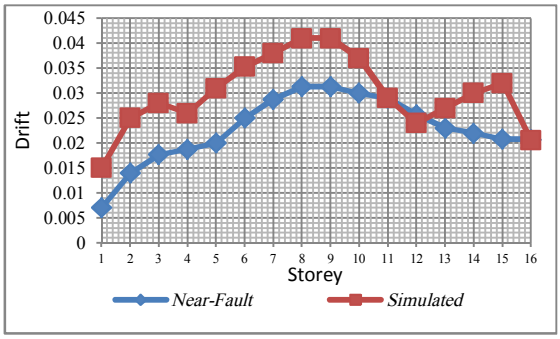

Kobe

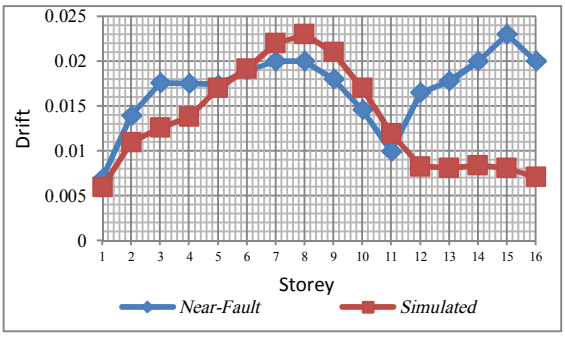

LomaPrieta

Fig 12. Maximum drift of stories for 16-story building under 7 near-fault and 7 simulated records

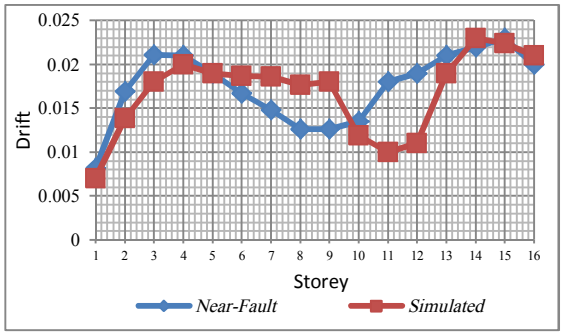

Northridge

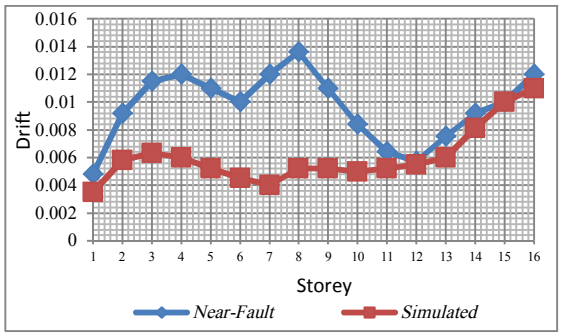

Parkfield

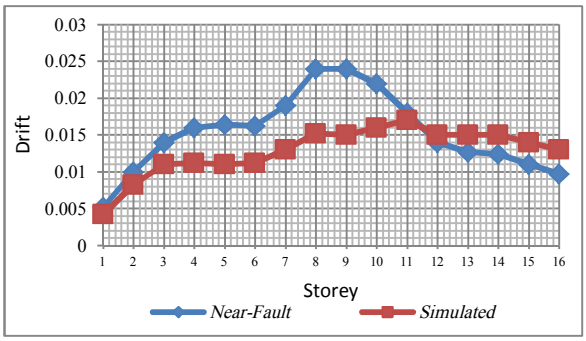

Superstation Hills

Fig.12. (Continue) Maximum drift of stories for 16-story building under 7 near-fault and 7 simulated records

7. Maximum inelastic base shear

Maximum inelastic base shear for the studied buildings subjected to near-fault earthquakes, and simulated records are represented in Fig. 13. Each twofold column shows maximum building base shear force for one near-fault record or its simulated record. Maximum inelastic base shear and maximum inelastic displacement of roof mass center happen almost simultaneously. In a 4-story building, maximum inelastic base shear and maximum inelastic displacement of roof mass center happen at the same time; however, as the height of the studied building increases, the time interval between maximum inelastic base shear and maximum inelastic displacement of roof mass center also increases. Maximum inelastic base shear in simulated and near-fault records happened simultaneously most of the time. In 4 and 8-story buildings, time interval happened completely close to each other and in 12 and 16-story buildings, it sometimes happened simultaneously and sometimes with a time lag.

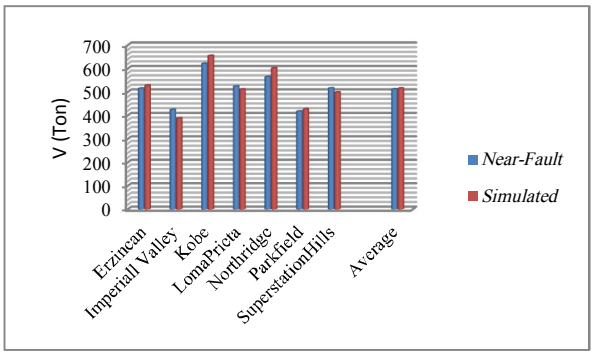

4 Story

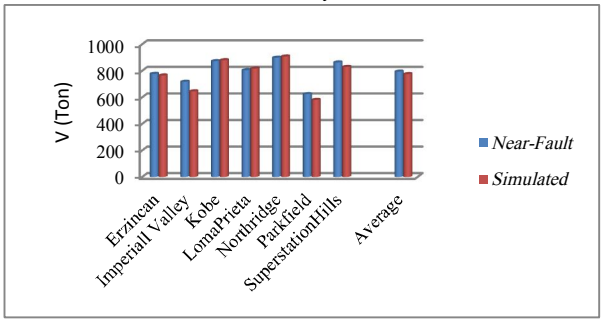

8 Story

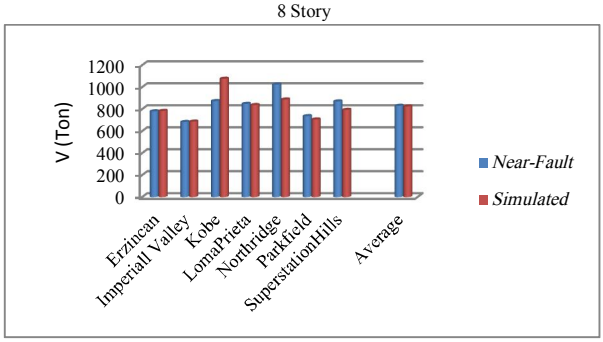

12 Story

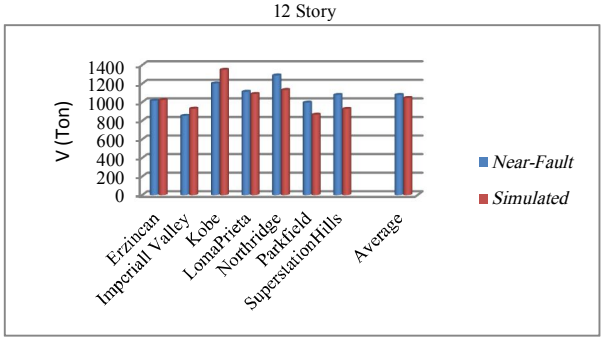

16 Story

Fig.13. Maximum inelastic base shear of studied buildings under near-fault and simulated records

8. Conclusion

The major purpose of the study was to probe whether the structures' responses to near-fault earthquakes with forward directivity have peculiar characteristics which distinguish such movements from common earthquakes. This response clearly represents pulse-type characteristics. This study characterized that simulated earthquakes can be used instead of near-fault ones. But it should be kept in mind that response spectrum of both near-fault and simulated records are mostly similar at a certain earthquake.

1. Generally, drift angle of near-fault earthquakes at low rise buildings is more than higher buildings. This is true at simulated records.
2. Maximum inelastic base shear happens when near-fault and simulated records have the maximum displacement.
3. All low rise buildings under several near-fault records have the same type of behavior and also the same type of stories drift. However, as the height of the building increases, the structure behavior and stories' drift become more divergent. This case is also true in simulated records.
4. To obtain maximum inelastic displacement, velocity and acceleration of roof mass center and also the structure's maximum inelastic base shear under near-fault records, simulated records can be used; but with the increase in structure height, the accuracy of the work decreases. Moreover, for obtaining maximum stories' drift under near-fault records, at shorter buildings (4-story buildings) simulated records can be used. However, as the height increases, the simulated records errors increase so that in 12-story buildings, the error grows and in some cases a more different behavior is observed.
5. In obtaining structures' non-linear response under simulated records, a simulated record generally has errors. So for convergence of response, several simulated records should be used (at least 7 records) and the average of obtained responses should be used.
6. In general, in the study of buildings less than 10 stories, the use of simulated records is recommended rather than near-fault records. Also due to increase in degrees of freedom and higher modes effects, in buildings more than 10 stories, structure response and behavior under the two above-mentioned records would be more different.

References

[1]Somerville P, Smith N, Graves R, Abrahamson N. Modifi--cation of empirical strong motion attenuation relations to include the amplitude and duration effects of rupture directivity. Seismological Society Letters 1997; 68(1):180-203

[2]Somerville P. Development of an improved ground motion representation for near-fault ground motion. SMIP98 seminar on utilization of strong-motion data, Oakland, CA, Sept, 1998.

[3] Malhotra P.K. Response of buildings to near-field pulse-like ground motions. Earthquake Engng.Struct.Dyn. 28, 1309-1326(1999).

[4] Bolt BA .Earthquakes. New York: W.H. Freeman; 1993.

[5]Stewart JP, Chiou S, Bray J, Graves R, Somerville P, Abrah- -amson N. Ground motion evaluation procedures for performance-based design. Pacific Earthquake Engineering Research Center (PEER), Report no.09, Sept, 2001.

[6] Bozorgnia B, Bertero V. Earthquake engineering: from engineering seismology to performance-based engineering. Florida: CRC Press; 2004.

[7]lavi B, Krawinkler H. Effects of near-fault ground motions on frame structures. The John A. Blume Earthquake Engineering Research Center, Report No. 138, Feb. 2001.

[8]Mahin S, Bertero V, Chopra A, Collins R. Response of the Olive View Hospital Main Building During the San Fernando Earthquake, Earthquake engineering research center, University of California, Berkeley, Report no. UCB/EERC- 76/22, Oct, 1976.

[9]Bertero V, Mahin S, Herrera R. Aseismic Design Impli--cations of near-fault San Fernando Earthquake Records, Earthquake Engng. Struct. Dyn, Vol. 6, Jan-Feb. 1978, 31-42.

[10] Anderson J.C ,Naeim F. Design criteria and ground motion effects in the seismic response of multi-story buildings , Proc. Applied Technology Council, ATC 10-1 , Seminar on Earthquake Ground Motion and Building Damage Potential, San Francisco, 1984.

[11] Hall J, Heaton T, Halling M, Wald D. Near-source ground motion and its effects on flexible buildings. Earthquake Spectra 1995; 11(4):569-605.

[12]Makris N. Rigidity-plasticity-viscosity: canelectrorheolog- -ical dampers protect base-isolated structures from near-source ground motions? Earthquake Engng.Struct.Dyn, 1997; 26: 571-91.

[13] Chopra A.K, Chintanapakdee C. Accuracy of response spe- - ctrum estimates of structural response to near-field earthquake ground motions: preliminary results, ASCE Structures World Conf., San Francisco, Paper no. T136-1 , 1998.

[14]Bozorgnia Y, Mahin S.A. Ductility and strength demands of near-fault ground motions of the Northridge earthquake. In: proceedings of the 6th US national conference on earthquake engineering, Seattle, Washington, 1998.

[15] Baker JW. Quantitative classification of near-fault ground motions using Wavelet analysis. Bulletin of seismological society of America 2007;97(5):1486-501.

[16] Sigurosson, S. U. 2010. MSc Thesis – Near-Fault Ground Motions and Structural Design Issues. School of Science and Engineering, Reykjavik .

[17] Champion, C. and Liel, A. 2012. The effect of near-fault directivity on building seismic collapse risk. Earthquake Engineering and Structural Dynamics 2012; 10.1002/eqe. 1188.

[18] Goto, R. 2012. Master Thesis- Seismic performance of a bridge subjected to far-field ground motions by a Mw 9.0 earthquake and near-field ground motions by a Mw 6.9 earthquake. Department of Civil and Architectural Engineering, Division of Structural Engineering and Bridges, Stockholm, Sweden.

[19] Iranian national building regulations, Tenth subject: design and performance of steel buildings (2008).

[20] Iranian national building regulations, Sixth subject: loads imposed on building (2009).

[21] Buildings design against earthquake: Iran 2800 earthquake code (Third Edition).

[22] Instruction for seismic rehabilitation of existing buildings: No 360, Islamic Republic of Iran Management and Planning Organization (2006)